FINITE ELEMENT ANALYSIS OF TENSILE LOAD RESISTANCE OF MORTISE-AND-TENON JOINTS CONSIDERING TENON FIT EFFECTS

Wengang Hu
PhD Student
College of Furnishings and Industrial Design
Nanjing Forestry University
Nanjing 210037, China
E-mail: 107318107@qq.com

*Huiyuan Guan**
Professor
College of Furnishings and Industrial Design
Nanjing Forestry University
Nanjing 210037, China
E-mail: hwg@njfu.edu.cn

Jilei Zhang†
Professor
Department of Forest Products
Mississippi State University
Mississippi State, MS 39762
E-mail: jzhang@cfr.msstate.edu

(Received June 2017)

Abstract. Effects of tenon fit in its width direction on the tensile load-deflection behavior of T-shaped, round-end, mortise-and-tenon joints were investigated experimentally and analytically. Finite element method (FEM) 3D modeling technique as an analytical tool was used to model the tensile load-deformation behavior of T-shaped, round-end, mortise-and-tenon joints. Experimental results indicated that mean ultimate tensile loads and stiffness of evaluated mortise-and-tenon increased significantly as tenon fit increased from 0 to 0.2 mm with an increment of 0.1 mm. The measured glue-line thickness between mortise-and-tenon contact surface was found to be a good indicator of tensile load resistance performance of mortise-and-tenon joints evaluated in this study. FEM modeling technique was verified as a valid analytical tool for prediction of tensile load resistances of T-shaped, round-end, mortise-and-tenon joints.

Keywords: Mortise-and-tenon joints, tensile load resistance, glue-line thickness, finite element method.

INTRODUCTION

The blind type of mortise-and-tenon joint is commonly used in wooden furniture construction, especially, in chairs, connecting critical structural members such as side rails to posts and stretchers to posts as shown in Fig 1. The joints connecting these critical members often resist an external load applied to a chair frame through internal reactive bending moments, shear forces, and axial tensile forces acting together (Eckelman 1978). The factors affecting strength performance of mortise-and-tenon joints include tenon fit (Hill and Eckelman 1973; Zhong and Guan 2007; Džinčić and Skakic 2012; Džinčić and Živanić 2014; Wang and Lee 2014), tenon shape and geometry (Hill and Eckelman 1973; Tankut and Tankut 2005), adhesive type and applying method (Hill and Eckelman 1973; Smardzewski 2002; Ratnasingam and Iorasn 2013), wood species (Smardzewski 2008; Derikvand and Smardzewski 2013), and wood MC. The effects of these factors on strength performance of mortise-and-tenon joints had been incorporated into prediction equations derived through regression

* Corresponding author
† SWST member

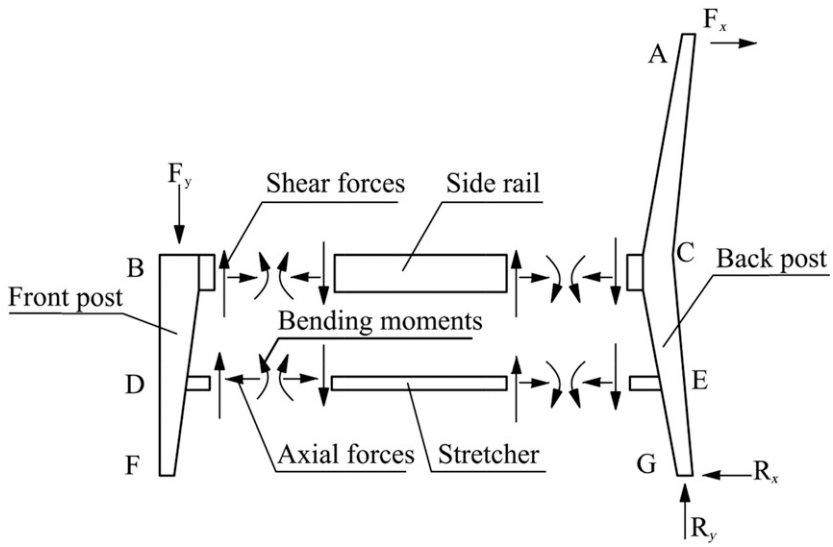

Figure 1. An example of a chair side frame shows internal reactive bending moments, shear forces, and axial forces acting simultaneously at critical joints of the chair frame subjected to external forces.

technique using experimental data (Hill and Eckelman 1973).

With the rapid development of computer technology and finite element theory, the finite element method (FEM) had been introduced into structure analysis of wood products and wooden constructions gradually (Mackerle 2005). The main road blocks limiting FEM usage in wooden structures, especially, in furniture frame structural analyses in the past, were mainly because of lack of right FEM elements, for instance, bonding elements for modeling interfacial bonding behavior of glued joints and also elastic properties of wood materials as an orthotropic engineering material (Smardzewski and Papuga 2004). In some studies, the solid wood was treated as an isotropic material instead of an orthotropic material, which was not able to reflect the real mechanical behaviors of wood (Bulent et al 2016). Gavronski (2006) and Çolakoglu and Apay (2012) used FEM to analyze the strength performance of a complete furniture frame with the assumption of mortise-and-tenon joints used in the structural model being rigid. Smardzewski and Papuga (2004) realized that it was difficult to build a reasonable structural model using FEM without the information related to joint properties. The glue-line thickness was considered as one of significant factors on strength and stiffness properties of mortise-and-tenon joints (Smardzewski 2008; Silvana and Smardzewski 2010; Kasal et al.2016), but no systematical research had been carried out.

There might be an immediate need for performing structural analyses of a furniture frame using FEM approach to obtain optimal design solution because using solid modeling technique to design a furniture frame is a common practice in furniture industry, but performing the structural analysis of a furniture frame using FEM technique with consideration of performing stress analyses at critical joints is not there yet. This is because limited studies were found in modeling the load-deformation behavior of a glued mortise-and-tenon joint using FEM technique with available newly developed bonding elements, especially, the load deformation of a glued mortise-and-tenon joint subjected to simple tensile load.

The main objective of this study was to investigate the load-deformation behavior of a T-shaped, round-end, mortise-and-tenon joint subjected to a tensile load experimentally and analytically. Therefore, specific objectives of this

study were to 1) measure elastic and strength properties of beech wood used for joint members, 2) investigate tenon fit on the shear strength of glued block samples cut from assembled joints with different tenon fits experimentally, 3) model the tensile load-deformation behavior of a T-shaped, round-end, mortise-and-tenon joint assembled with different tenon fits using FEM technique, and 4) validate the FEM model experimentally. It was expected that the outcomes from this study could contribute to our knowledge of continuously searching the solution of making FEM technique as a practical structural analysis tool for the furniture industry.

MATERIALS AND METHODS

Experimental Design

Mortise-and-tenon joints. Figure 2(a) shows the general configuration of a T-shaped mortise-and-tenon joint specimen used in this study. The joint consisted of a stretcher with its end attached to a post through round-end mortise-and-tenon construction applied with polyvinyl acetate emulsion (PVAc) adhesive of 52% solids content. The post and stretcher were constructed of beech (*Fagus orientalis Lipsky*). The stretcher measured 120 mm long × 40 mm wide × 30 mm thick. The post measured 150 mm long × 40 mm wide × 30 mm thick. All joint members were prepared from quartersawn lumber (Fig 2[b]). The mortise measured 16 mm wide × 30 mm high × 30 mm deep.

A one-way complete factorial experiment with 20 replications was conducted to evaluate the tensile load resistance of T-shaped mortise-and-tenon joints. The factor was tenon fit in its width direction (ie the difference between tenon width and mortise height as shown in Fig 2[b]) and the tenon fit had three levels of 0, 0.1, and 0.2 mm. The tenon fit in its thickness direction (ie the difference between tenon thickness and mortise width) was a negative constant of 0.2 mm.

Basic mechanical properties. Figure 3 illustrates sizes, grain orientations, and strain gauges locations of samples used for evaluating compressive yield strength and moduli of elasticity (E_L, E_R, E_T) and their corresponding Poisson ratios (υ_{LR}, υ_{LT}, υ_{RT}, υ_{RL}, υ_{TR}, υ_{TL}), as well as moduli of rigidity (G_{LT}, G_{LR}, and G_{RT}) of beech wood for joint member materials. Ten replicates

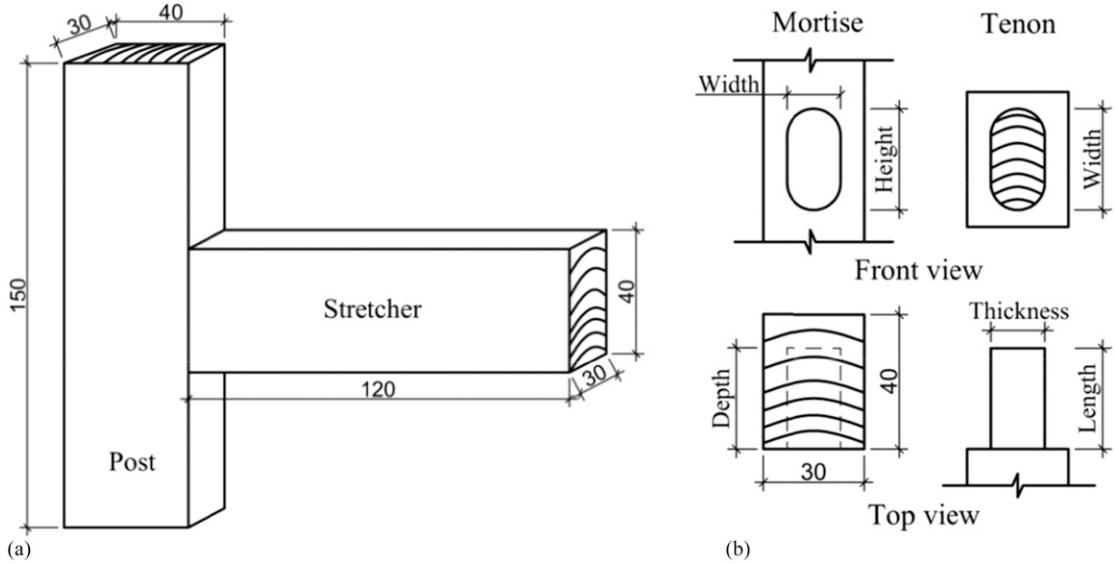

Figure 2. The configuration of a typical specimen (a) used in this study for evaluating tensile loads of T-shaped mortise-and-tenon joints, and detailed shapes and dimensions (unit: mm) of mortise-and-tenon (b).

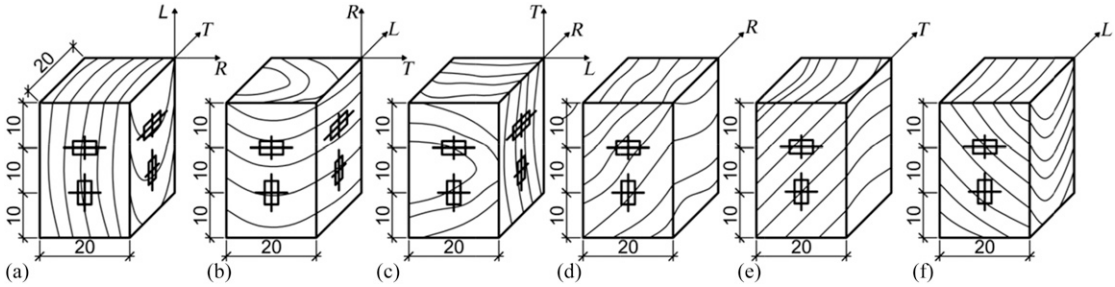

Figure 3. The sizes and grain orientations of wood specimens for obtaining elastic moduli and Poisson's ratios of E_L, V_{LR}, V_{LT} (a), E_R, V_{RT}, V_{RL} (b), and E_T, V_{TR}, V_{TL} (c), and shear modulus of G_{LT} (d), G_{LR} (e), and G_{RT} (f).

were tested for compressive strengths in longitudinal, radial, and tangential directions with specimens shown in Fig 3(a)-(c) without strain gauge, respectively. Ten replicates were tested for each of three moduli of elasticity and each of three moduli of rigidity, respectively. In addition, specific gravity and MC of wood materials were measured with 20 replicates.

Bonding shear strength. Figure 4(e) shows the configuration of a shear block sample and the location where the sample was cut from a mortise-and-tenon joint specimen (Fig 4[a] and [b]). Twenty shear blocks were cut from each of three assembled joint groups evaluated for tenon fit effects, respectively. The shear strength of tested blocks was calculated using the following equation:

$$\tau = P/(a \times b),$$

where τ is the shear strength of glued block samples ($N \cdot mm^{-2}$), P is the ultimate loading force (N), a is the bonding surface width (mm), and b is the bonding surface length (mm).

Glue-line thickness. The glue used for analyzing the glue-line thickness of mortise-and-tenon joints was a mixture of 10 parts (liquid weight) of PVAc glue and one part of urea formaldehyde (UF) resin. This is because PVAc adhesive cannot be stained with dyes but UF resin can be. Figures 4(c) and (d) show the configurations of glue-line samples and the locations where they were cut from mortise-and-tenon specimens (Fig 4[a] and [b]). The reason for cutting specimen blocks from two different locations of the joints, ie one with curved contact surface (Fig 4[c]) and the other with flat contact surface (Fig 4[d]), was that it was believed that the actual pressures applied on the contact surfaces of these two blocks would be different because of tenon fit effects. Three joints were prepared for each of three clearances.

Specimen Preparation

Before joint member cutting operation, all member materials were conditioned in a room with temperature controlled at 22°C and the RH at 48%. All joint members were cut by computer numerical control machine with an accuracy of 0.01 mm (Yuanli, China). An adhesive was liberally coated on both tenon and mortise surfaces right after machining operation. The amount of applied adhesive was controlled at 182 ± 25 g/m^2 through gravimetric method. All specimens were stored in a room with the temperature controlled at 22°C and the RH at 48% for a week before testing.

Testing

Basic mechanical properties. All elastic property tests of beech materials were performed on an universal testing machine instrumented the data acquisition instrument (TDS530, TML, Tokyo, Japan) in reference to the procedures outlined in the literature (Murata and Tanahashi

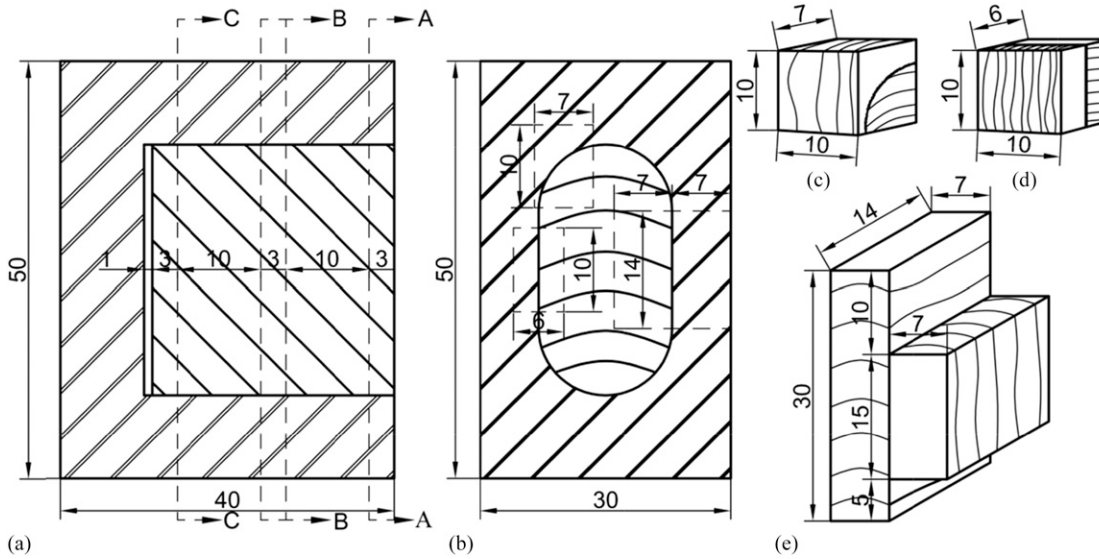

Figure 4. The cutting pattern (a, b) for preparing samples for glue-line thickness measurement (c, d) and glue shear strength testing (e).

2010; Aira et al 2014; Hu and Guan 2017a). The physical properties of beech wood were determined in accordance with the procedures described in ASTM (2001).

Shear strength of bonded blocks. All shear tests were performed on a 20 kN capacity universal testing machine at a loading rate of 1 mm/min (CNS 2013), and the testing setup was illustrated in Fig 5. Ultimate shear loads and failure modes were recorded for all tested shear blocks.

Joint tensile loads. All joint tensile tests were carried out on an universal testing machine (SHIMADZU, Nakagyo-ku, Japan) at a loading rate of 10 mm/min, and the testing setup was illustrated in Fig 6. The test continued until the joints were disabled. Load-displacement curves of all tested joints and their failure modes were recorded.

Glue-line thickness measurement. Fluorescence microscope (DM 50008B, Leica, Shanghai, China) was used to analyze the actual glue-line thickness of joints assembled with three different tenon fits. Toluidine blue solution with 0.5% solid content was used to stain all block specimens. The glue-line thickness of all specimens was measured using Imagine J2x software.

Modeling

Figure 7 is the model created using Abaqus software (ref) for evaluating the tensile load of a T-shaped mortise-and-tenon. Geometry, loading, and boundary conditions of the model were based on Figs 2 and 6. Required inputs for elastic

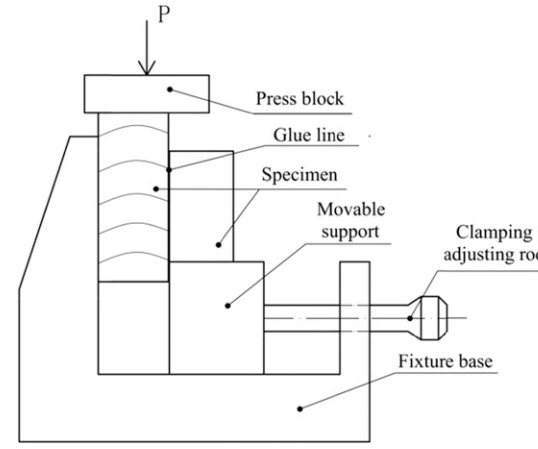

Figure 5. Diagram illustrating test setup for evaluating shear strength of glued block specimens.

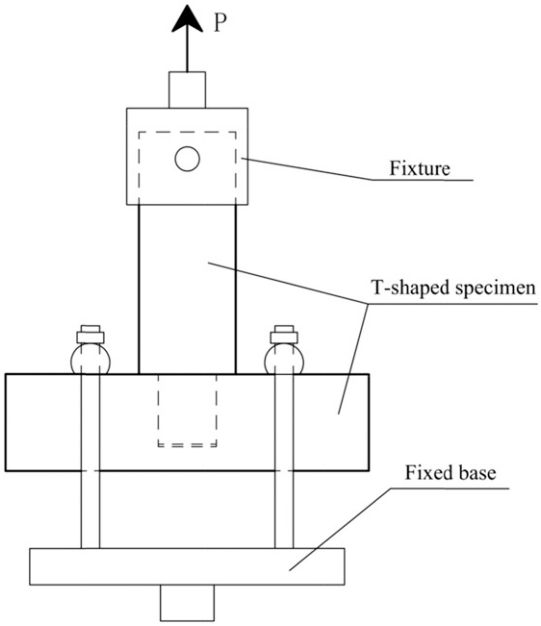

Figure 6. Diagram showing the setup for measuring tensile loads of T-shaped mortise-and-tenon joints in this study.

properties of beech wood were three moduli of elasticity, three moduli of rigidity, and six Poisson's ratios as orthotropic material, and for glue line, they were one modulus of elasticity and one Poisson's ratio as isotropic material. Material strength properties required for inputs were compressive strengths in longitudinal, tangential, and radial directions, respectively, and shear strength of glue bonding. Elastic properties of beech wood were measured in this experiment, whereas elastic properties of PVAc glue line were from literature (Kasal et al 2016), ie the modulus of elasticity was 460 MPa and Poisson's ratio was 0.3. In general, 3D element, C3D8R, was used to model wood materials, specifically, the element size of 1.4 mm × 1.4 mm × 1.4 mm was used for the material close to the contact surfaces of mortise-and-tenon and the element size of 5 mm × 5 mm × 5 mm was used for the rest of joint member materials. Curve surfaces of mortise-and-tenon joints were modeled using 3D element, C3D8R, and surface-to-surface contact property was friction with their surface friction coefficient set to 0.54 (Hu and Guan 2017b). The reason for using nonbonding element for

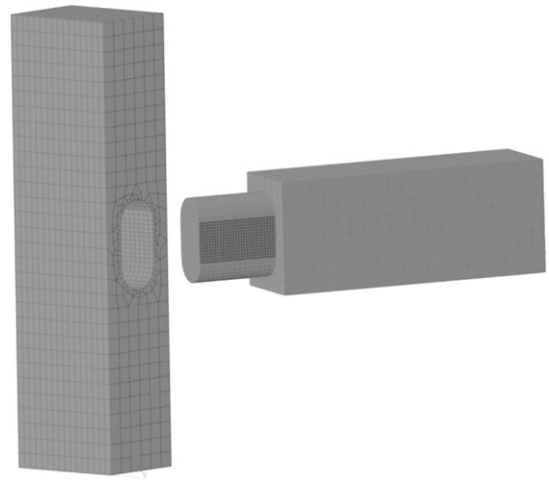

Figure 7. Finite element model created for analyzing tensile loads and shear stress distributions of T-shaped mortise-and-tenon joints evaluated in this study.

modeling curved surface was because in the actual experiment, it was observed that there was lack of adhesive in the contact surfaces of the curved area. Cohesive element, COH3D8, with the size of 1 mm × 1 mm × 1 mm, was used to model the glue line between flat surfaces of mortise-and-tenon joints, and the glue-line thickness was set based on fluorescence microscope analysis results. A 30-mm displacement was imposed to the end of the stretcher to produce a pulling out effect on the joint model. The total reaction force obtained at the boundary was the tensile load of the modeled joint.

Statistical Analyses

All mean comparisons were performed at the 5% significance level using the protected least significant difference (LSD) multiple comparisons procedure.

RESULTS AND DISCUSSION

Basic Material Properties

The specific gravity and MC of joint member materials averaged 0.62 with its coefficient of variation (COV) of 0.84% and 10.8 with its COV of 1.5%, respectively. Table 1 summarizes the

Table 1. Summary of mechanical properties of solid beech wood measured in this study.

Modulus of elasticity			Poisson's ratio						Shear modulus			Yield strength		
E_L (Mpa)	E_R (Mpa)	E_T (Mpa)	υ_{LR}	υ_{LT}	υ_{RT}	υ_{TR}	υ_{TL}	υ_{RL}	G_{LR} (Mpa)	G_{LT} (Mpa)	G_{RT} (Mpa)	L (Mpa)	T (Mpa)	R (Mpa)
12,205	1858	774	0.502	0.705	0.526	0.373	0.038	0.078	899	595	195	42.51	4.49	9.83

twelve elastic constants and yield strengths in three grain orientations measured for solid beech wood used in this study. Mean shear strength values of glued blocks cut from mortise-and-tenon joints are summarized in Table 2.

These elastic constants and strength properties were used as material property data input into the FEM modeling.

Table 2 shows that there was an increase trend observed for shear strength mean values of glued block as tenon fit increased from 0 to 0.2 mm with an increment of 0.1 mm. But, the results of mean comparisons performed using the single LSD value of 0.625 MPa indicated that these increases were not significant.

Tensile Loads

Figure 8 shows typical load-displacement curves of T-shaped mortise-and-tenon joints resulted from experimental testing and FEM modeling. Table 2 summarizes mean ultimate tensile loads and stiffness constants of tested mortise-and-tenon joints and their corresponding analytical values predicted using FEM method. The ratios between analytical and experimental ultimate tensile load values ranged from 0.89 to 0.97. These results indicated that in general FEM modeling technique could be used to reasonably estimate ultimate tensile loads of T-shaped mortise-and-tenon joints evaluated in this study, even though it tended to underestimate ultimate tensile loads of the joints. The ratios between analytical and experimental stiffness values ranged from 3.2 to 4.2, which indicated that the stiffness of a FEM modeled joint tended to be much stiffer than its actual joint specimen. Further study needs to investigate effects of element size and glue-line elastic property on the stiffness behavior of a mortise-and-tenon joint modeled using FEM technique.

Mean comparison results (Table 2) indicated that ultimate tensile loads and stiffness of evaluated mortise-and-tenon increased significantly as tenon fit increased from 0 to 0.2 mm with an increment of 0.1 mm. These mean comparison results were performed using the single LSD value of 265 N and 491 N/mm, for ultimate tensile load and stiffness values, respectively. The significantly higher ultimate tensile load of a mortise-and-tenon joint with a larger tenon fit than a smaller tenon fit could be partially explained by the fact that the larger tenon fit joint had a higher interfacial bonding strength in terms of shear strength measured for the glued block cut from mortise-and-tenon joints (Table 2) than the smaller one.

Glue-Line Thickness

Figure 9 shows typical fluorescence microscope images of glued blocks cut from mortise-and-tenon joint specimens for glue-line thickness analyses. There was no obvious glue line observed in curved contact surfaces of mortise-and-tenon

Table 2. Summary of mean values of glue-line thickness and shear strength measured for shear blocks cut from joint samples, and mean ultimate tensile loads and stiffness of mortise-and-tenon joints measured experimentally and estimated analytically.

Tenon fit (mm)	Glue-line thickness (μm)	Shear strength (MPa)	Ultimate tensile load			Stiffness		
			Experimental (N)	Analytical (N)	Ratio	Experimental (N/mm)	Analytical (N/mm)	Ratio
0	97.54	3.267 (17.5) A	3155 (11.6) C	2996	0.95	3594 (12.85) C	11,311	3.2
0.1	75.74	3.489 (18.7) A	4434 (5.7) B	3939	0.89	4129 (15.46) B	16,481	4.0
0.2	55.51	3.776 (22.4) A	5133 (4.3) A	4998	0.97	4757 (11.02) A	19,921	4.2

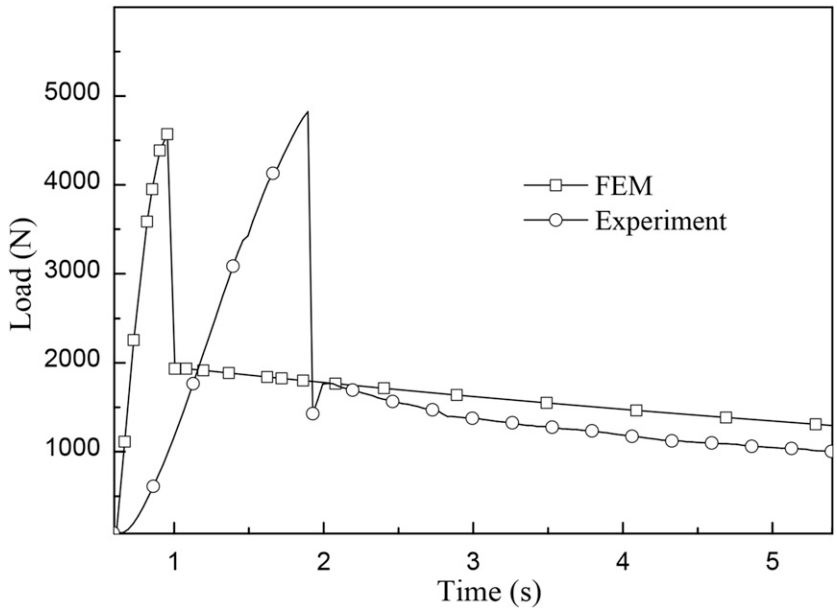

Figure 8. Typical experimental and analytical load-displacement curves of T-shaped mortise-and-tenon joints evaluated in this study. FEM, finite element method.

joints (Fig 9[a]). This phenomenon of absence of glue at curved contact surfaces of joints was consistent with the observation carried out by Džinčić and Živanić (2014).

Clear glue line (Fig 9[b]) was observed in all flat contact surfaces of mortise-and-tenon joints, and mean glue-line thickness values of all flat contact surface samples were summarized in Table 2. There was a decrease trend in glue-line thickness as tenon fit increased from 0 to 0.2 mm, but the decrease seems not significant. The decrease in glue-line thickness as tenon fit increased would be explained by the fact that the tenon thickness can be expanded under the compression of tenon in its width direction (Fig 2[b]) because of tenon oversized in its width direction comparing to mortise height. This size expansion of tenon in its thickness can cause the increase of pressure between two flat contact surfaces of mortise-and-tenon joints evaluated in this study. Furthermore, this pressure increase can lead to good glue penetration to open wood cells and therefore a good interfacial bonding between two flat contact surfaces of mortise-and-tenon joint, resulting in a higher shear strength of glued surfaces and a higher tensile load resistance of mortise-and-tenon joints. These could explain why mean ultimate tensile loads of evaluated mortise-and-tenon joints increased significantly as tenon fit increased from 0 to 0.2 mm with an increment of 0.1 mm.

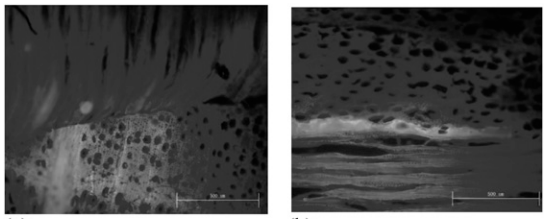

Figure 9. Fluorescence microscope images of typical glue lines observed between mortise-and-tenon surfaces contacted at curved (a) and flat (b) regions of mortise-and-tenon joints evaluated in this study, respectively.

Joint Failure Mode and Stress Distribution

Figure 10 shows three typical failure modes observed on tenon surfaces of mortise-and-tenon

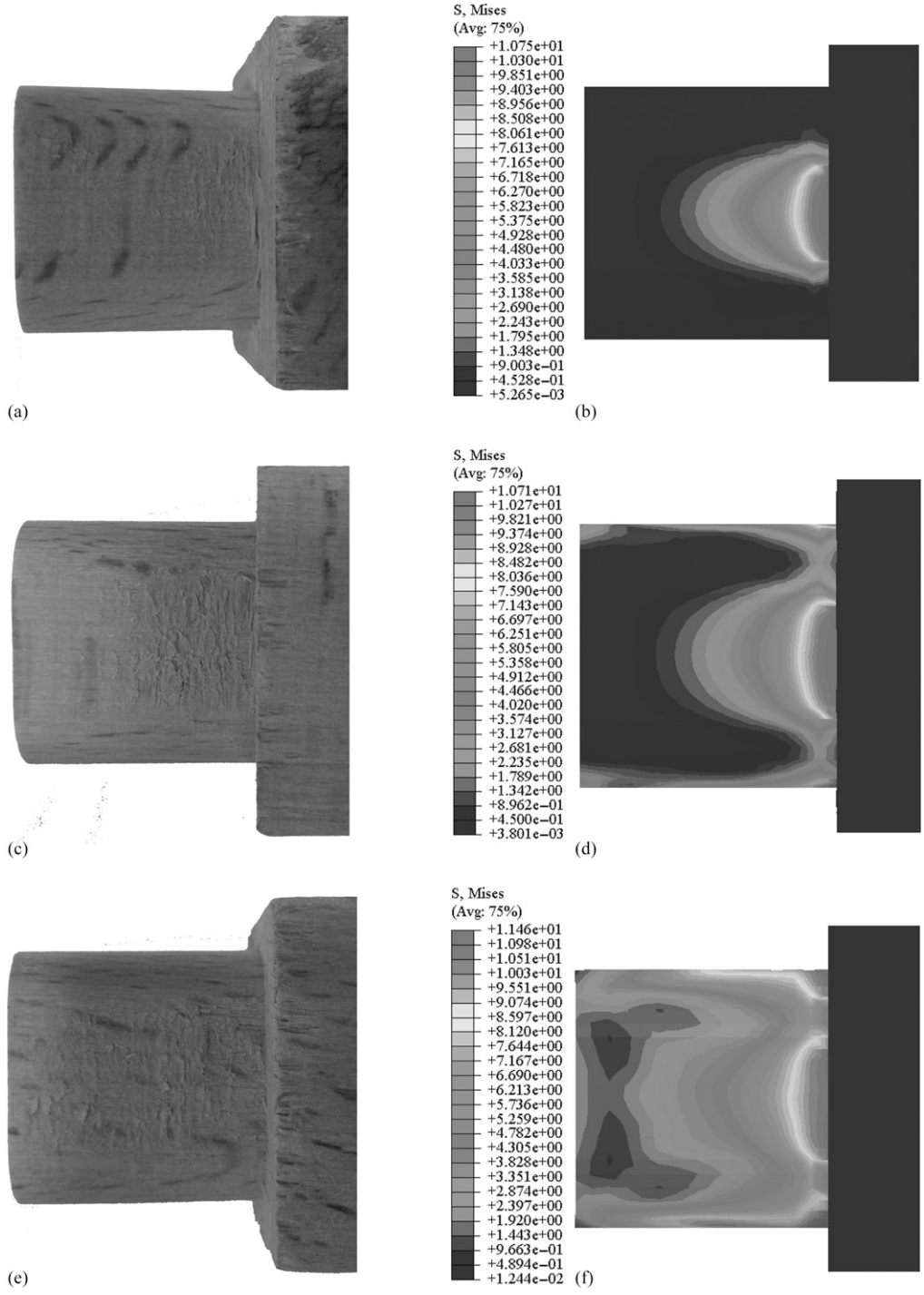

Figure 10. Typical joint failure modes observed on tenons of evaluated mortise-and-tenon joints assembled with tenon fits of 0 (a), 0.1 (c), and 0.2 (e) mm, and analytical shear stress distributions corresponding to each of tenon fits, 0 (b), 0.1 (d), and 0.2 (f) mm, respectively.

joints tested in this study and analytical shear stress distributions corresponding to each of three failure modes. The fractured area of interfacial bonding observed on tenon surfaces (Fig 10[a], [c], and [e]) increases as tenon fit increases from 0 to 0.2 mm with an increment of 0.1 mm. This increase trend of fractured area on tenon surfaces matches shear stress contour patterns which indicate that the joints with the larger tenon fit tend to have a relatively uniformly distributed shear stress pattern, ie showing less stress concentration on the interfacial bonding surface of mortise-and-tenon joints. This uniformly distributed shear stress pattern on tenon surfaces explained why the joint with a larger tenon fit had a significantly higher tensile load resistance than the one with a smaller tenon fit because the tensile load calculated using the uniformly distributed stress pattern (Fig 10[f]) will be significantly higher than the one using less uniformly distributed pattern (Fig 10[d]).

All aforementioned discussion implies that there is an optimal tenon fit in general for construction of mortise-and-tenon joints that can result an optimal pressure applied on two flat contact surfaces of a mortise-and-tenon. This pressure can lead to the highest shear strength resulted in between two glued surfaces of mortise-and-tenon joints. Eventually, the highest shear strength will result in the highest tensile load resistance of a mortise-and-tenon joint.

CONCLUSIONS

The major conclusions from experimental and analytical results of this study on tensile load resistance performance of round-end mortise-and-tenon joints are following:

1) Tenon fit in its width direction had significant effects on the ultimate tensile load resistance and stiffness of round-end mortise-and-tenon joints. Mean ultimate tensile loads and stiffness of evaluated mortise-and-tenon in this study increased significantly as tenon fit increased from 0 to 0.2 mm with an increment of 0.1 mm. The increase in ultimate tensile loads of mortise-and-tenon joints was because the oversize of joint tenon in its width caused the size expansion in its thickness direction which resulted in pressure increase between mortise-and-tenon flat contact surfaces and led to a good interfacial bonding and uniformly distributed shear stress between the flat contact surfaces of mortise-and-tenon joints.
2) Glue-line thickness can be a good indicator in evaluating tensile load resistance performance of glued, round-end, mortise-and-tenon joints because it is related to how much pressure is applied to the contact surfaces of glued joints and also how uniformly shear stress is distributed on the interfacial bonding surface of glued mortise-and-tenon joints.
3) FEM modeling technique can be used to model and predict the ultimate tensile load resistance reasonably, but the model tends to overestimate joint stiffness. Further investigation needs in FEM modeling of stiffness performance of T-shaped, round-end, mortise-and-tenon joints.

ACKNOWLEDGMENT

This study was supported by a project funded by A Priority Academic Program Development of Jiangsu Higher Education Institutions (PAPD).

REFERENCES

Aira JR, Arriaga F, González GL (2014) Determination of the elastic constants of scots pine (*Pinus sylvestris* L.) wood by means of compression tests. Biosyst Eng 126:12-22.

ASTM (2001) Standard test methods for direct moisture content measurement of wood and wood-base materials. D 4442-92. American Society for Testing and Materials, West Conshohocken, PA.

Bulent K, Huseyin Y, Burhanettin U (2016) Simulating strength behaviors of corner joints of wood constructions by using finite element method. Drv Ind 67(2):133-140.

CNS (2013) Determination of shear strength on bonded assembly of solid wood for furniture. QB/T 1903-2013. China National Standard, Beijing, China.

Çolakoglu MH, Apay AC (2012) Finite element analysis of wooden chair strength in free drop. Int J Phys Sci 7(7):1105-1114.

Derikvand M, Smardzewski J (2013) Withdrawal force capacity of mortise and loose tenon T-type furniture joints. Turk J Agric For 37:469-478.

Džinčić I, Skakic D (2012) Influence of type of fit on strength and deformation of oval tenon-mortise joint. Wood Res Slovakia 57(3):469-477.

Džinčić I, Živanić D (2014) The influence of fit on the distribution of glue in oval tenon/mortise joint. Wood Res Slovakia 59(2):297-302.

Eckelman CA (1978) Strength design of furniture. Tim Tech, Inc., West Lafayette, IN.

Gavronski T (2006) Rigidity-strength models and stress distribution in housed tenon joints subjected to torsion. Electron J Pol Agric Univ Wood Technology 9(4), #32. http://www.ejpau.media.pl/volume9/issue4/art-32.html.

Hill MD, Eckelman CA (1973) Flexibility and bending strength of mortise and tenon joints. *In* Furniture design and manufacturing, Vol. 45, No. 1 and 2, Dun-Donnelley Corp., Chicago, IL.

Hu WG, Guan HY (2017a) Investigation on withdrawal capacity of mortise and tenon joint based on friction properties. Linye Gongcheng Xuebao 2(04):158-162 (in Chinese with summary in English).

Hu WG, Guan HY (2017b) Study on elastic modulus of beech in different stress states. Linye Gongcheng Xuebao 2(06):36-41 (in Chinese with summary in English).

Kasal A, Smardzewski J, Kuskun T, Erdil YZ (2016) Numerical analyses of various sizes of mortise and tenon furniture joints. BioResources 11(3):6836-6853.

Mackerle J (2005) Finite element analyses in wood research: A bibliography. Wood Sci Technol 39(7):579-600.

Murata K, Tanahashi H (2010) Measurement of Young's modulus and Poisson's ratio of wood specimens in compression test. J Soc Mater Sci Jpn 59(4):285-290.

Ratnasingam J, Iorasn F (2013) Effect of adhesive type and glue-line thickness on the fatigue strength of mortise and tenon furniture joints. Eur J Wood Wood Prod 71(1):819-821.

Silvana P, Smardzewski J (2010) Effect of glue line shape on strength of mortise and tenon joint. Drv Ind 61(4): 223-228.

Smardzewski J (2002) Strength of profile-adhesive joints. Wood Sci Technol 36(2):173-183.

Smardzewski J, Papuga T (2004) Stress distribution in angle joints of skeleton furniture. Electron J Pol Agric Univ Wood Technology 7(1), #05. http://www.ejpau.media.pl/volume7/issue1/wood/art-05.html.

Smardzewski J (2008) Effect of wood species and glue type on contact stresses in a mortise and tenon joint. J Mec Eng Sci 222(12):2293-2299.

Tankut AN, Tankut N (2005) The effects of joint forms (shape) and dimensions on the strengths of mortise and tenon joints. Turk J Agric For 29:493-498.

Wang YR, Lee SH (2014) Design and analysis on interference fit in the hardwood dowel glued joint by finite element method. Procedia Eng 79:166-172.

Zhong SL, Guan HY (2007) Relationship between optional value of interference fit and wood density in oval tenon joint. China For Sci Technol 21(02):57-59 (in Chinese with summary in English).